



Cite this: *Dalton Trans.*, 2015, **44**, 484

Received 1st October 2014,  
Accepted 11th November 2014  
DOI: 10.1039/c4dt03029j

www.rsc.org/dalton

## Photogeneration of two reduction-active charge-separated states in a hybrid crystal of polyoxometalates and naphthalene diimides†

Jian-Jun Liu,<sup>a</sup> Yao Wang,<sup>a</sup> Mei-Jin Lin,<sup>\*a,b</sup> Chang-Cang Huang<sup>\*a</sup> and Wen-Xin Dai<sup>a</sup>

**The combination of naphthalene diimide tectons with zinc cations in the presence of polyanions, Mo<sub>6</sub>O<sub>19</sub><sup>2-</sup>, leads to a hybrid crystal composed of two-dimensional porous coordination networks and polyoxometalates, which can generate two kinds of long-lived charge-separated states for the reduction reactions upon irradiation.**

Photocatalysis has seen growing interest, not only in the reactions of small molecules such as H<sub>2</sub>O (water splitting)<sup>1</sup> and CO<sub>2</sub> (forming solar fuels),<sup>2</sup> but also in organic transformation.<sup>3</sup> Similar to natural photosynthesis, one of the most striking aspects in this work is the photogeneration of stable charge-separated states in the catalysts for the further photo-induced electron transfer (PICT) reactions. Due to the energy level difference between components that always results in an intercomponent electron transfer, few available photocatalysts, particularly inorganic–organic ones involve in two kinds of oxidation-active or reduction-active charge-separated states. That is, both of them are for the selective oxidation or reduction reactions of a substrate, which is of considerable realistic significance because it avoids multi-step catalytic reactions for those containing several functional groups.<sup>4</sup> To this end, an obvious strategy is to use two components with close energy levels in one system. However, the selection of two photoactive inorganic and organic species and then fabrication into one is no easy matter.

Naphthalene diimides<sup>5</sup> (NDIs) are an attractive class of electron-deficient n-type organic semiconducting molecules, whose LUMO energy levels are in a small range of  $-4.32$  to

$-3.22$  eV and always serve as electron acceptors in the PICT processes.<sup>6</sup> Poly-oxometalates<sup>7</sup> (POMs) are a distinctive class of nanosized anionic metal oxygen clusters that exhibit good redox and photo-activity, and can not only act as electron donors but also acceptors for the PICTs since their LUMO energy levels vary from  $-4.31$  eV of Lindqvist-type Mo<sub>6</sub>O<sub>19</sub><sup>2-</sup> to  $1.87$  eV of Keggin-type PMo<sub>12</sub>O<sub>40</sub><sup>3-</sup>.<sup>8</sup> From the standpoint of energy levels, there is every reason to believe that both naphthalene diimides and the Mo<sub>6</sub>O<sub>19</sub><sup>2-</sup> anion can play as electron acceptors in one system if they are in the presence of sufficiently electron-rich donors. More importantly, the electronic complementarity between NDIs and POMs (anion– $\pi$  interactions<sup>9</sup>) provides a driven force to fabricate them into an inorganic–organic hybrid.<sup>10</sup> Herein, we reported that this design principle is indeed viable.

For the realization of this principle, the facile *N,N'*-di(4-pyridyl)-1,4,5,8-naphthalene diimide (DPNDI)<sup>11</sup> has been selected in spite of the slightly higher LUMO energy level ( $-3.72$  eV<sup>6a</sup> for core-unsubstituted NDIs) than that of the Mo<sub>6</sub>O<sub>19</sub><sup>2-</sup> polyanion ( $-4.31$  eV<sup>8b</sup>), which is because its coordination interplay with metal cations has been reported to increase its  $\pi$ -acidity and thus lower its LUMO energy level.<sup>12</sup> A further reason is that the aforementioned interplay with metal cations can also lead to porous cationic coordination networks that will somewhat balance the anionic charge of inorganic photochromic polyoxometalates. Furthermore, the generated porous coordination networks can provide enough cavity space to include polyoxometalates and other substrates for further photocatalytic applications. For the sufficiently electron-rich donors, *N*-methylpyrrolidin-2-one (NMP) was used, which is mainly because of its good solubility in DPNDI, together with the fact that it is a known electron donor for the photo-induced electron transfer of POMs.<sup>13</sup> As expected, the combination of DPNDIs with zinc fluorosilicate (ZnSiF<sub>6</sub>) in the presence of giant anions, Mo<sub>6</sub>O<sub>19</sub><sup>2-</sup>, led to a hybrid [Zn(DPNDI)<sub>2</sub>(NMP)<sub>2</sub>](Mo<sub>6</sub>O<sub>19</sub>) (1), in which two kinds of long-lived charge-separated states for the reduction reactions, Mo<sup>5+</sup> in POMs and radicals in NDI units, have been generated upon irradiation.

<sup>a</sup>State Key Laboratory of Photocatalysis on Energy and Environment, College of Chemistry, Fuzhou University, 350116, China. E-mail: meijin\_lin@fzu.edu.cn, cchuang@fzu.edu.cn

<sup>b</sup>State Key Laboratory of Structural Chemistry, Fujian Institute of Research on the Structure of Matter, Chinese Academy of Sciences, 350002, China

†Electronic supplementary information (ESI) available: Experimental details, TGA and PXRD plots, crystallographic data (CIF), photographs, and XPS. CCDC 1022530. For ESI and crystallographic data in CIF or other electronic format see DOI: 10.1039/c4dt03029j

Yellow crystals of **1** were obtained in quantitative yields upon slow diffusion of MeOH solution of  $\text{ZnSiF}_6 \cdot 6\text{H}_2\text{O}$  into NMP solution of DPNDI and  $(n\text{-Bu}_4\text{N})_2[\text{Mo}_6\text{O}_{19}]$  with a buffered layer of a mixed solution of MeOH and NMP (1 : 1 in volume). The combination was investigated by the X-ray diffraction technique on single crystals, which revealed that it is crystallized in the monoclinic space group of  $C2/c$  and consists of cationic NDI zinc coordination networks and  $\text{Mo}_6\text{O}_{19}^{2-}$  polyanions (Fig. 1). Specifically, each smallest repetitive unit of **1** is composed of one zinc cation, two bridged DPNDI units, two coordinated NMP molecules and one  $\text{Mo}_6\text{O}_{19}^{2-}$  polyanion. For other free solvents, they are disordered in the formed voids and unfortunately not all of them could be refined. Thus, their contributions have been subtracted from the data using SQUEEZE during the crystallographic refinement.<sup>14</sup>

In the crystal, each zinc cation adopts an octahedral geometry coordinated with four N atoms from four DPNDI tectons in the square plane ( $d_{\text{Zn-N}} = 2.13\text{--}2.18 \text{ \AA}$ ,  $\angle\text{N-Zn-N} = 87.1\text{--}94.9^\circ$ ) and two O atoms from two NMP molecules in axial positions ( $d_{\text{Zn-O}} = 2.11\text{--}2.17 \text{ \AA}$ ,  $\angle\text{O-Zn-O} = 177.4^\circ$ ) to yield a mononuclear complex (Fig. 1a), which is further bridged by DPNDI linkers to form a cationic two-dimensional network with a square grid of  $19.79 \text{ \AA} \times 19.79 \text{ \AA}$  (Fig. 1b). Along the  $a$  axis, the neighbouring two networks are slightly slipped and bridged by  $\text{Mo}_6\text{O}_{19}^{2-}$  polyanions at the corner of square grids through the anion- $\pi$  ( $d_{\pi\text{-O}} = 3.04\text{--}3.43 \text{ \AA}$ ) and  $\text{CH}\cdots\text{anion}$  interactions ( $d_{\text{C-O}} = 3.33\text{--}3.63 \text{ \AA}$ , Fig. 1c) to form a three-dimensional hybrid structure with the distances between neighbouring two network planes of around  $5.69 \text{ \AA}$ , while those between neighbouring

two zinc centres of  $9.20\text{--}9.35 \text{ \AA}$  (Fig. 1d and 1e). In other words, the neighboring two DPNDIs from the neighboring two networks are interconnected side-to-side through the formation of  $\text{CH}\cdots\text{O}$  hydrogen bonds ( $d_{\text{C-O}} = 3.32\text{--}4.26 \text{ \AA}$ ,  $\angle\text{C-H}\cdots\text{O} = 137.9\text{--}159.8^\circ$ , Fig. 1c) resulting in a three-dimensional network bearing rhombic nanotube channels with hydrogen-bonding NDI ribbons as a tube wall. In each tube, the  $\text{Mo}_6\text{O}_{19}^{2-}$  anions bitten by two DPNDI units through anion- $\pi$  and  $\text{CH}\cdots\text{anion}$  interactions are padded alternately at the two opposite cores. It is worth pointing out that the close distances between the coordinated NMP and DPNDI units are less than  $3.5 \text{ \AA}$  ( $d_{\text{C-O}} = 3.04\text{--}3.21 \text{ \AA}$ ,  $d_{\text{C-C}} = 3.48 \text{ \AA}$ ), and those between C atoms in NMP molecules and O atoms in polyanions are in the range of  $3.37\text{--}3.60 \text{ \AA}$ , which is supposed to play a very important role in their electron separation and transfer upon the external light stimuli (see below).

The purity of the crystalline materials generated has been investigated by X-ray diffraction on powder samples (Fig. S3, ESI†). The latter study reveals that almost only one phase has been observed for hybrid **1** because of a rather good fit between its simulated and observed patterns. The slight discrepancy is attributed to the trace collapsed crystalline materials upon removal of the solvent molecules, which is further supported by its thermogravimetric analysis. The thermal behavior of **1** has been investigated under a nitrogen atmosphere in the temperature range of  $35\text{--}800 \text{ }^\circ\text{C}$ . As shown in Fig. S2,† less than 2% weight loss is observed under  $100 \text{ }^\circ\text{C}$ , indicating that hybrid **1** contains few low-boiling-point solvent molecules. In the temperature range of  $100\text{--}200 \text{ }^\circ\text{C}$ , *ca.* 13% weight loss is attributed to the loss of crystalline free NMP solvents that have been removed using SQUEEZE during its structural refinement. Then almost no weight loss is observed until about  $290 \text{ }^\circ\text{C}$  in which a sharp weight loss of around 10% is observed, which may come from the loss of coordinated NMP molecules (calculated value: 9.3%). After this, other components and the framework also begin to decompose gradually.

The color and electron absorption spectral changes are two important features to probe whether photo-induced charge separations occur in a material. As expected of the design principle, the hybrid crystal **1** undergoes a photochromic transformation from yellow to dark green upon irradiation by sunlight or a 365 nm UV light (11 W) (Fig. 2a, inset), which becomes darker and darker when the irradiation time is increased. The generated dark green crystals are rather stable in air (Fig. S3 and S4†) but can return to yellow in a dark room after three days at ambient temperature. X-Ray crystallography revealed that the dark green crystal is identical to **1**. Similar color-changing has already been reported in NDI based coordination networks,<sup>15</sup> indicating that a photo-induced radical generation for NDI units may occur, which is confirmed by the solid-state UV/Vis diffuse reflectance spectral (DRS) studies. As shown in Fig. 2a, upon irradiation by a 365 nm UV light for 30 minutes, a new broad band with an absorption maximum at around 630 nm, which can be assigned to NDI radical species, is indeed observed in the DRS spectra, accompanied

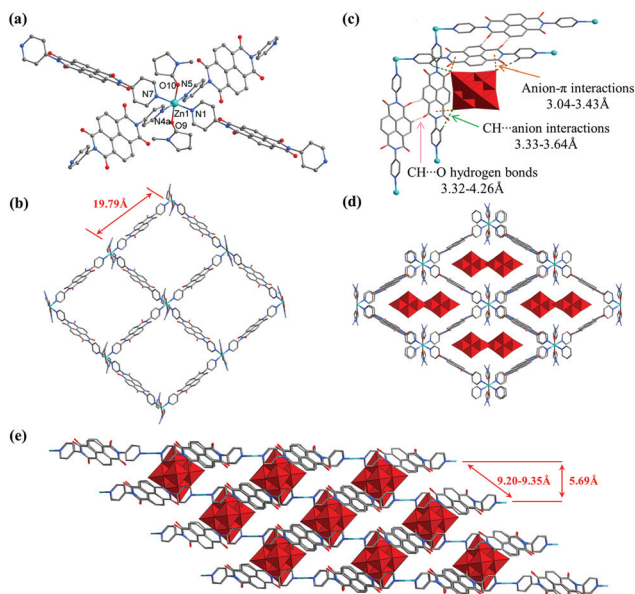


**Fig. 1** (a) Coordination environment of  $\text{Zn}^{2+}$  in complex **1** (symmetry codes:  $a: 0.5 + x, 0.5 - y, -0.5 + z$ ); (b) two-dimensional coordination network; (c) the interactions between NDI units and  $\text{Mo}_6\text{O}_{19}^{2-}$  polyanion; (d–e) top and side views of the coordination naphthalene diimide grids including polyoxometalates in cavities. For clarity, all the H atoms except for those highlighting C–H $\cdots$ anion interactions and C–H $\cdots$ O hydrogen bonds in (c), as well as NMP molecules in (e) are omitted.

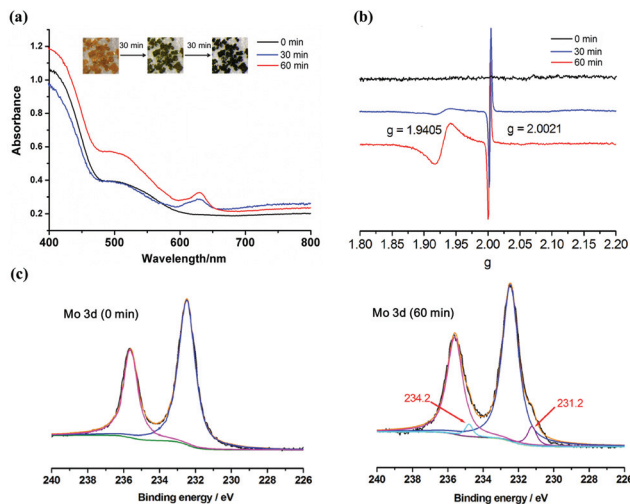


**Fig. 2** (a) UV/Vis spectral changing of complex **1** upon irradiation by a 365 nm UV light (0, 30 and 60 minutes, 11 W), the inset shows the photochromic effect of a single crystal from photographic images; (b) ESR spectra of complex **1** before and after irradiation; (c) XPS core level Mo(3d) spectra of complex **1** before and after irradiation.

by the decrease of the absorption band of neutral NDI species (400–460 nm). Surprisingly, upon irradiation for another 30 minutes, such a newly generated NDI radical absorption band is just slightly enhanced. Instead, another broad band with absorption maximum at around 510 nm assigned to  $\text{Mo}^{5+} \rightarrow \text{Mo}^{6+}$  intervalence charge transfer,<sup>13c,16</sup> increases much more, which implies that two kinds of charge-separated states,  $\text{Mo}^{5+}$  in POMs and radicals in NDI units, are supposed to form in crystal **1**. This speculation is unequivocally substantiated by the electron spin resonance (ESR) and X-ray photoelectron spectroscopy (XPS) studies.

As shown in Fig. 2b, due to ESR silence, no clear paramagnetic signal is observed for hybrid **1**. However, upon irradiation for 30 minutes, other than a sharp and intense signal at  $g = 2.0021$  assigned to NDI radicals, another broad and weak signal at  $g = 1.9405$  is also observed in the ESR spectrum. Interestingly, only the latter increases upon irradiation for another 30 minutes (Fig. 2b). With reference to the previous studies,<sup>13c,17</sup> this paramagnetic signal at  $g = 1.9405$  is attributed to the formation of  $\text{Mo}^{5+}$ , which is further corroborated by X-ray photoelectron spectroscopy. As depicted in Fig. 2c, two main peaks of the 3d shell for Mo atoms at 235.6 eV and 232.5 eV, corresponding to their  $3d_{3/2}$  and  $3d_{5/2}$  of  $\text{Mo}^{6+}$  cations,<sup>18</sup> can be detected in the core-level spectra, which become broader after irradiation for 60 minutes, wherein, two new small peaks at 234.2 eV and 321.2 eV with lower binding energy, assigned to those of  $\text{Mo}^{5+}$  cations, can be separated successfully by peak-resolution techniques. For the Zn  $2p_{3/2}$  and C 1s, almost the same XPS patterns are found, indicating no electron gain or loss for both atoms upon irradiation (Fig. S1, ESI†). Due to the complicated bonding environment, the O 1s and N 1s spectra of hybrid **1** could not be separated. From the above UV/Vis and ESR studies, two reduction active

sites (NDI radical and  $\text{Mo}^{5+}$ ) are generated sequentially. That is, NDI radicals are formed first from the neutral NDI units by accepting electrons from the coordinated NMP molecules, followed by  $\text{Mo}^{5+}$  in POMs, indicating that the LUMO energy level of the NDI unit is slightly lower than that of the  $\text{Mo}_6\text{O}_{19}^{2-}$  polyanion. As expected, the coordination indeed could lower the LUMO energy levels of the NDI ligands. Considering the coexistence of the formed NDI radical and  $\text{Mo}^{5+}$ , their energy levels should also be close and unfavorable to the mutual electron transfer but favorable to the electron exchange. In addition, such electron exchange is supposed to play a key role in the long life time of two charge-separated states, particularly for  $\text{Mo}^{5+}$ . For NDI radicals, the long life time is further related to the close-contacting NDI ribbon structure (Fig. 1b), which favors the electron transport.

It is known that both the reduced-state  $\text{Mo}^{5+}$  and NDI radicals are reduction-active, which can return to stable  $\text{Mo}^{6+}$  and neutral NDIs by transferring one electron to the oxidizers. As stated above, the color of crystal **1** upon irradiation for 60 minutes can be recovered by standing in a dark room for three days at ambient temperature, which may be attributed to the oxidation of the generated  $\text{Mo}^{5+}$  and NDI radicals by  $\text{O}_2$  in air. Actually, such recovery can be greatly accelerated upon the addition of more oxidative sodium nitrite aqueous solution ( $0.1 \text{ mmol L}^{-1}$ ) (within 2 hours, Fig. S5†).

In summary, we have reported a hybrid crystal composed of two-dimensional porous naphthalene diimide based coordination networks and polyoxometalates, which can generate two kinds of long-lived charge-separated states for the reduction reactions upon irradiation. Such photogenerated stable charge-separated states are of considerable realistic significance, e.g. for the photocatalytic reactions of the substrates containing several functional groups. Further research on this domain is in progress.

We thank Prof. Jun-Dong Wang for his useful discussions and Prof. Zhao-Hui Li for assistance with the ESR measurement. This work was supported by the National Natural Science Foundation of China (21202020 and 21273037), the Doctoral Fund of Ministry of Education of China (20123514120002), the Natural Science Foundation of Fujian Province (2014J01040 and 2014J01045), and the Science & Technical Development Foundation of Fuzhou University (2012-XQ-10 and 2013-XQ-14).

## Notes and references

- (a) J. Xing, W. Q. Fang, H. J. Zhao and H. G. Yang, *Chem. – Asian J.*, 2012, **7**, 642–657; (b) M. Yagi and M. Kaneko, *Chem. Rev.*, 2001, **101**, 21–36; (c) J. P. McEvoy and G. W. Brudvig, *Chem. Rev.*, 2006, **106**, 4455–4483; (d) H. Lv, Y. V. Geletii, C. Zhao, J. W. Vickers, G. Zhu, Z. Luo, J. Song, T. Lian, D. G. Musaev and C. L. Hill, *Chem. Soc. Rev.*, 2012, **41**, 7572–7589; (e) P. Zhang, J. Zhang and J. Gong, *Chem. Soc. Rev.*, 2014, **43**, 4395–4422.

- 2 (a) S. N. Habisreutinger, L. Schmidt-Mende and J. K. Stolarczyk, *Angew. Chem., Int. Ed.*, 2013, **52**, 7372–7408; (b) Y. Ma, X. Wang, Y. Jia, X. Chen, H. Han and C. Li, *Chem. Rev.*, 2014, **114**, 9987–10043; (c) A. J. Cowan and J. R. Durrant, *Chem. Soc. Rev.*, 2013, **42**, 2281–2293; (d) Y. Oh and X. Hu, *Chem. Soc. Rev.*, 2013, **42**, 2253–2261.
- 3 (a) J. Xuan and W.-J. Xiao, *Angew. Chem., Int. Ed.*, 2012, **51**, 6828–6838; (b) S. Sumino, A. Fusano, T. Fukuyama and I. Ryu, *Acc. Chem. Res.*, 2014, **47**, 1563–1574; (c) C. K. Prier, D. A. Rankic and D. W. C. MacMillan, *Chem. Rev.*, 2013, **113**, 5322–5363; (d) J. M. R. Narayanam and C. R. J. Stephenson, *Chem. Soc. Rev.*, 2011, **40**, 102–113.
- 4 (a) X. Xu, P. Y. Zavalij, W. Hu and M. P. Doyle, *Chem. Commun.*, 2012, **48**, 11522–11524; (b) F. Frusteri, M. Cordaro, C. Cannilla and G. Bonura, *Appl. Catal., B*, 2015, **162**, 57–65; (c) B.-L. Li, H.-C. Hu, L.-P. Mo and Z.-H. Zhang, *RSC Adv.*, 2014, **4**, 12929–12943.
- 5 (a) S. V. Bhosale, C. H. Jani and S. J. Langford, *Chem. Soc. Rev.*, 2008, **37**, 331–342; (b) N. Sakai, J. Mareda, E. Vauthey and S. Matile, *Chem. Commun.*, 2010, **46**, 4225–4237; (c) F. Würthner and M. Stolte, *Chem. Commun.*, 2011, **47**, 5109–5115; (d) S. Bhosale, V. S. V. Bhosale and S. K. Bhargava, *Org. Biomol. Chem.*, 2012, **10**, 6455–6468.
- 6 (a) Z. Liu, G. Zhang, Z. Cai, X. Chen, H. Luo, Y. Li, J. Wang and D. Zhang, *Adv. Mater.*, 2014, **26**, 6965–6977; (b) H. Luo, Z. Cai, L. Tan, Y. Guo, G. Yang, Z. Liu, G. Zhang, D. Zhang, W. Xu and Y. Liu, *J. Mater. Chem. C*, 2013, **1**, 2688–2695; (c) T. B. Singh, S. Erten, S. Günes, C. Zafer, G. Turkmen, B. Kuban, Y. Teoman, N. S. Sariciftci and S. Icli, *Org. Electron.*, 2006, **7**, 480–489.
- 7 (a) M. T. Pope, *Heteropoly and Isopoly Oxometalates*, Springer, Berlin, 1983; (b) L. Cronin and A. Müller, *Chem. Soc. Rev.*, 2012, **41**, 7333–7334; (c) H. N. Miras, J. Yan, D.-L. Long and L. Cronin, *Chem. Soc. Rev.*, 2012, **41**, 7403–7430; (d) S. T. Zheng and G. Y. Yang, *Chem. Soc. Rev.*, 2012, **41**, 7623–7646; (e) R. C. Snoberger III, K. J. Young, J. Tang, L. J. Allen, R. H. Crabtree, G. W. Brudvig, P. Coppens, V. S. Batista and J. B. Benedict, *J. Am. Chem. Soc.*, 2012, **134**, 8911–8917.
- 8 (a) C. L. Hill, D. A. Bouchard, M. Kadkhodayan, M. M. Williamson, J. A. Schmidt and E. F. Hilinski, *J. Am. Chem. Soc.*, 1988, **110**, 5471–5479; (b) L.-K. Yan, S.-Z. Wen, J.-P. Wang and Z.-M. Su, *Comput. Theor. Chem.*, 2012, **988**, 1–5; (c) Y.-R. Guo, Q.-J. Pan, Y.-D. Wei, Z.-H. Li and X. Li, *J. Mol. Struct. (THEOCHEM)*, 2004, **676**, 55–64.
- 9 (a) H. T. Chifotides and K. R. Dunbar, *Acc. Chem. Res.*, 2013, **46**, 894–906; (b) B. L. Schottel, H. T. Chifotides and K. R. Dunbar, *Chem. Soc. Rev.*, 2008, **37**, 68–83; (c) Y. Zhao, C. Beuchat, Y. Domoto, J. Gajewy, A. Wilson, J. Mareda, N. Sakai and S. Matile, *J. Am. Chem. Soc.*, 2014, **136**, 2101–2111; (d) J.-Z. Liao, X.-J. Dui, H.-L. Zhang, X.-Y. Wu and C.-Z. Lu, *CrystEngComm*, 2014, **16**, 10530–10533.
- 10 (a) T. Yamase, *Chem. Rev.*, 1998, **98**, 307–325; (b) C. Sanchez, B. Julian, P. Belleville and M. Popall, *J. Mater. Chem.*, 2005, **15**, 3559–3592; (c) M.-S. Wang, G. Xu, Z.-J. Zhang and G.-C. Guo, *Chem. Commun.*, 2010, **46**, 361–376; (d) R. Pardo, M. Zayat and D. Levy, *Chem. Soc. Rev.*, 2011, **40**, 672–687.
- 11 (a) S. Guha, F. S. Goodson, R. J. Clark and S. Saha, *CrystEngComm*, 2012, **14**, 1213–1215; (b) S. Guha, F. S. Goodson, L. J. Corson and S. Saha, *J. Am. Chem. Soc.*, 2012, **134**, 13679–13691.
- 12 (a) X. Fang, X. Yuan, Y.-B. Song, J.-D. Wang and M.-J. Lin, *CrystEngComm*, 2014, **16**, 9090–9095; (b) D. Quiñonero, A. Frontera and P. M. Deyà, *ChemPhysChem*, 2008, **9**, 397–399.
- 13 (a) L.-Z. Zhang, W. Gu, X. Liu, Z. Dong and B. Li, *CrystEngComm*, 2008, **10**, 652–654; (b) L.-Z. Zhang, W. Gu, Z. Dong, X. Liu, B. Li and M.-L. Liu, *J. Solid State Chem.*, 2009, **182**, 1040–1044; (c) H. Zhang, L. Duan, Y. Lan, E. Wang and C. Hu, *Inorg. Chem.*, 2003, **42**, 8053–8058.
- 14 A. L. Spek, *Acta Crystallogr., Sect. D: Biol. Crystallogr.*, 2009, **65**, 148–155.
- 15 L. Han, L. Qin, L. Xu, Y. Zhou, J. Sun and X. Zou, *Chem. Commun.*, 2013, **49**, 406–408.
- 16 (a) E. B. Wang, L. Xu and C. W. Hu, *Chin. Sci. Bull.*, 1991, **20**, 1544; (b) M. T. Pope, *Mixed-Valence Compounds, Heteropoly Blues*, Reidel, Oxford, 1979.
- 17 (a) K. Hakouk, O. Oms, A. Dolbecq, H. E. Moll, J. Marrot, M. Evain, F. Molton, C. Duboc, P. Deniard, S. Jobic, P. Mialane and R. Dessapt, *Inorg. Chem.*, 2013, **52**, 555–557; (b) V. T. T. Ha, A. Sarıođlan, A. Erdem-Şenatalar and Y. B. Taârit, *J. Mol. Catal. A: Chem.*, 2013, **378**, 279–284.
- 18 M. Anwar, C. A. Hogarth and R. Bulpett, *J. Mater. Sci.*, 1990, **25**, 1784–1788.